Ion Currents and Membrane Domains in the Cleaving *Xenopus* Egg

DOUGLAS KLINE, KENNETH R. ROBINSON, and RICHARD NUCCITELLI
Department of Zoology, University of California, Davis, California 95616; and Department of Physiology, University of Connecticut Health Center, Farmington, Connecticut 06032

ABSTRACT We used an extracellular vibrating probe to measure ion currents through the cleaving *Xenopus laevis* egg. Measurements indicate sharp membrane heterogeneities. Current leaves the first cleavage furrow after new, unpigmented membrane is inserted. This outward current may be carried by K^+ efflux. No direct involvement of the Na^+,K^+-ATPase in the generation of this outward current is detected at first cleavage. Inward current enters the old, pigmented membrane; however, it does not enter uniformly. The inward current is largest at the old membrane bordering the new membrane. This suggests a heterogeneous ion channel distribution within the old membrane. Experiments suggest that the inward current may be carried by Na^+ influx, Ca^{2+} influx, and Cl^- efflux. No steady currents were detected during grey crescent formation, the surface contraction waves preceding cleavage, or with groove formation at the beginning of cleavage.

The cleavage process in amphibian eggs includes the addition of new membrane at the cleavage furrow that forms blastomeres with two distinct membrane domains. Each blastomere retains some of the original egg surface with pigment granules underlying the membrane and each gains new, unpigmented membrane. In addition to being morphologically distinct, these membrane domains appear to have different electrical properties. Woodward (45) and de Laat and co-workers (7, 8) have suggested that the membrane hyperpolarization observed during first cleavage is due to the addition of new, unpigmented membrane that has a high potassium permeability. We investigated the electrical properties of these two membranes in *Xenopus laevis* embryos, using the extracellular vibrating probe that is used to measure steady ion currents which cells drive through themselves.

Ion currents have been shown to be correlated with growth and pattern formation in a number of developing systems (5, 19, 22, 23, 28, 44). In a previous study of immature *Xenopus* oocytes, Robinson (31) detected an animal-vegetal current which falls to nearly zero in response to a variety of maturation-promoting factors. No steady transmembrane currents have been detected in the mature, unfertilized egg or in precleavage fertilized eggs aside from a ring-shaped wave of inward current which spreads over the egg for 4 min following activation (D. Kline and R. Nuccitelli, manuscript in preparation). Here we report on electrical measurements made beginning 15 min after fertilization and on through second cleavage. Large steady currents are found after new membrane has been added at cleavage. We describe experiments and results that suggest which ions carry the current and discuss the significance of heterogeneous membranes and transcellular currents.

MATERIALS AND METHODS

Obtaining Eggs and Sperm: Eggs were obtained from *Xenopus laevis* females by injection of 800 IU of human chorionic gonadotropin (Sigma Chemical Company, St. Louis, MO) into the dorsal lymph sac. 8–14 h after injection eggs were fertilized in vitro by stripping the eggs from a female directly into a sperm suspension made from macerating a small piece of testis in the fertilizing medium. Eggs were fertilized in modified F1 solution (15) containing 41.25 mM NaCl, 1.75 mM KCl, 0.5 mM Na_2HPO_4, 1.9 mM NaOH, 2.5 mM HEPES, 0.25 mM $CaCl_2$, and 0.06 mM $MgCl_2$ at pH 7.8.

10–15 min after the addition of eggs to the sperm suspension the fertilization medium was removed and the fertilized eggs were dejellied in Steinberg's Solution (58.0 mM NaCl, 0.67 mM KCl, 0.3 mM $Ca(NO_3)_2$, 0.8 mM $MgSO_4$, and 5 mM Tris) with 1% papain and 0.2% cysteine at pH 8.0 for 1–2 min. Alternatively eggs were dejellied in modified F1 with 2% cysteine at pH 7.8 for 4–5 min or until all jelly coats were removed. The eggs were washed thoroughly by five to six complete changes of the medium. The fertilization envelope was left intact or was removed manually with watchmaker's forceps. All measurements using the vibrating probe were made in 5% De Boer's Ringer (5.5 mM NaCl, 0.07 mM KCl, 0.07 mM $CaCl_2$, and 2.0 mM tricine at pH 7.8) or in modified 5% De Boer's Ringer (as indicated in Table II).

Vibrating Probe Technique and Experimental Methods: The extracellular vibrating probe (Vibrating Probe Co., Davis, CA) can be used to measure steady electrical currents near living cells (21). The probe consists of a solder-filled electrode with a 10–30 μm platinum-black ball at its tip and a coaxial reference electrode 3 mm behind the tip. The probe is made

to vibrate by using a piezoelectric bender element to which is applied a sinusoidal voltage. The probe is connected to a lock-in amplifier (model 5204; Princeton Applied Research, Princeton, NJ). The lock-in amplifier acts as a voltmeter tuned to the vibration frequency and detects any voltage difference between the extremes of vibration. If there is a net flux of ions into or out of a cell, the movement will generate a local voltage gradient in the extracellular medium. Vibration of the probe converts any steady voltage difference into a sinusoidal output the amplitude of which is measured with the aid of the lock-in amplifier.

Over the small distance of vibration (20–40 μm) the electric field is nearly constant so it may be approximated by the voltage difference divided by the vibration amplitude. The current density at the center of vibration, in the direction of vibration, may then be calculated by dividing the voltage difference by the resistivity of the medium in which the probe is vibrated. 1 $\mu A/cm^2$ corresponds to a net ion flux of $\sim$10 pmol/cm^2-s.

To determine the current pattern around the fertilized egg and cleavage-stage embryo, we placed an egg in a small dish with 5% De Boer's Ringer on the stage of an inverted microscope. The vibrating probe was moved into position with the aid of an XYZ micropositioner (Line Tool Co., Allentown, PA). Fig. 1 *B* shows the probe in position over the cleavage furrow. The current pattern around the egg was obtained by placing the probe at a number of locations around the egg, recording the voltage signal and calculating the current density at each location. Two or usually three measurements were obtained for each position to check the reliability of the system and the variation in the current. All measurements were made at a room temperature of 20 ± 1°C.

To obtain information about the ionic composition of the current, we made measurements in modified 5% De Boer's Ringer with substitution of certain ions, with the addition of ion channel blockers, or with the addition of inhibitors of the Na^+,K^+-ATPase. Medium in the measuring dish was exchanged with the use of a double syringe system by which fluid was added and withdrawn at the same rate. 20 ml of medium was exchanged through a 3-ml chamber in 0.5 to 2 min and this disturbed neither the egg nor the vibrating probe. Before replacement of the medium at least three measurements were made at a single position near the egg. After changing the medium, the probe was returned as closely as possible to its original position by using an ocular reticle or the accurate micrometer of the XYZ micropositioner and three or more measurements were made again. The resistivities of the normal and each experimental medium were obtained by taking the inverse of the conductivity as given by a standard conductivity meter (ElectroMark Analyzer, Markson Science, Inc., Del Mar, CA).

The probe was calibrated and checked for maximum signal detection as needed. It is possible to record an artifactual voltage difference when the probe is held near an object due to current leaks from the probe vibrator or from corrosion batteries elsewhere in the system. These leakage currents can cause so-called "barrier artifacts" when they are reflected from a cell or another electrical barrier. Barrier artifacts are generally small in our present vibrating probe system. Before each experiment the probe was positioned near a glass ball approximately the size of the *Xenopus* egg. A typical example of the recordings obtained is shown in Fig. 2*A*. Over the course of these experiments the apparent echo current was often undetected. If detected the apparent current usually corresponded to a flow of positive ions into the barrier averaging 0.01 ± .02 $\mu A/cm^2$ (SD, $n = 27$).

Current densities cannot be recorded precisely at the cell membrane surface. Typically the midpoint of vibration is 60–100 μm from the surface. Values of current densities at the membrane surface must be obtained by extrapolation based on the nature of the fall-off in signal with increasing distance from the cell surface. The complex geometry of the cleaving egg makes it difficult to calculate a theoretical extrapolation factor. Current densities at the cell surface will generally be greater than at the probe position. However, for some geometries of the cleaving egg it is impossible to position the probe perpendicular to the cell surface and in these positions the measured current density might be smaller at the surface than in the measurement position. Current densities for all measurements are reported as measured at the probe position and the distance to the cell surface is indicated.

RESULTS

We have observed steady electrical currents in the cleavage stage *Xenopus laevis* embryo. We were able to begin measurements as early as 15 min after fertilization, after removal of the jelly coats and fertilization envelope. However, large steady currents were not observed until newly formed, unpigmented membrane was inserted into the cleavage furrow $\sim$7 min after the beginning of cleavage. This cleavage current will be described first. We will then describe our findings at later cleavages and prior to first cleavage and present some data on the ionic composition of the current.

First cleavage in *Xenopus* eggs begins with the formation of a single pigmented stripe at the animal pole, followed by the formation of a shallow groove with transverse stress lines. This groove advances down towards the vegetal pole as cleavage progresses. Groove formation in *Xenopus* and other amphibians has been associated with the presence of microfilaments in the cortical layer (26, 35, 37). We cannot detect steady transmembrane ion currents associated with groove formation.

Outward Current at the First Cleavage Furrow

An area of unpigmented, white membrane is added at the animal pole beginning $\sim$7 min after cleavage begins. We refer to this membrane as unpigmented membrane throughout this paper since it lacks the pigment granules that underlie the original egg membrane. The photograph in Fig. 1*A* shows unpigmented membrane in the cleavage furrow at first cleavage.

We detect a significant steady outward current at the new, unpigmented membrane when it is first observed at the cell

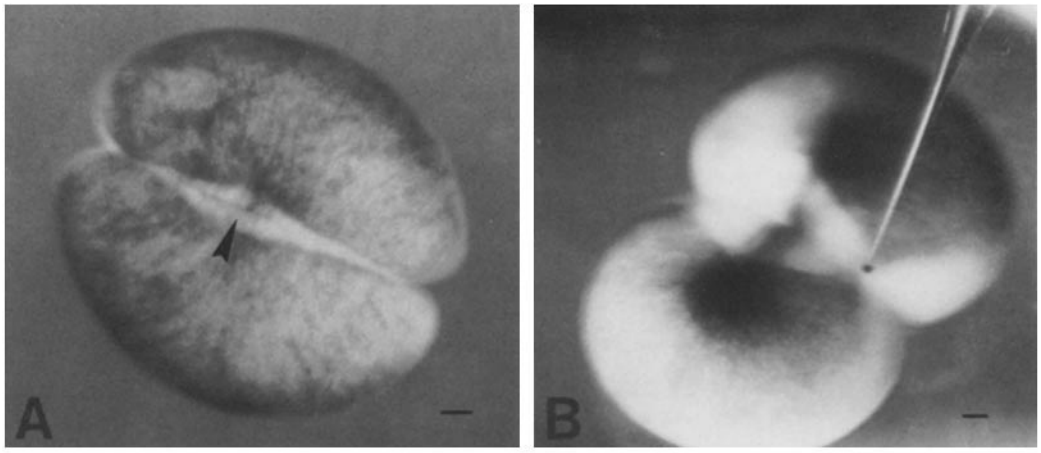

FIGURE 1 Photographs of cleaving *Xenopus laevis* eggs. (*A*) Photograph of a *Xenopus* egg during 1st cleavage in the fertilization envelope after removal of the jelly. Arrow shows new, unpigmented membrane in the plane of cleavage. Bar, 100 μm. × 45. (*B*) Photograph of a *Xenopus* egg during first cleavage after removal of the fertilization envelope. The vibrating probe (not vibrating) is shown in position above the cleavage furrow. Bar, 100 μm. × 45.

surface. This is most easily measured when the fertilization envelope is removed and the probe is positioned over the animal hemisphere as shown in Fig. 1*B*. Removal of the fertilization envelope results in slightly more blastomere separation and more new membrane is exposed; otherwise cleavage is normal. Current can be detected leaving the area of unpigmented membrane as soon as it becomes visible at the animal pole. The magnitude of this outward current increases as much as 10-fold as more new membrane appears during the 20-min period preceeding second cleavage. Outward current is always observed when the probe is vibrated horizontally in the plane of cleavage and opposite new, unpigmented membrane at the cleavage furrow. When the probe is positioned with the direction of vibration in the cleavage plane and raised 100–400 μm above the equator at the intersection of the cleavage plane and the vertical plane tangent to the edge of the forming blastomeres (the plane shown in Fig. 2*C*), outward current is usually measurable. When the fertilization envelope is removed the probe may be moved up from the equator and into the furrow (Fig. 2*C* probe position 3, and Fig. 1*B*). The magnitude of the recorded current increases as the probe is moved into the furrow. For example, probe position 3, in Fig. 2*C*, shows the current record for the outward current when the probe was positioned 300 μm above the equator and in the cleavage plane 270 μm from the vertical plane tangent to both blastomeres, ~150 μm from the cell surface at the center of the furrow. When positioned at this same height and between 100 and 400 μm from the cell surface at the furrow center, the mean maximum outward current was 0.43 ± .26 (SD, n = 29) μA/cm^2. Values ranged from 0.13 to 1.18 μA/cm^2 depending on the particular egg and distance between the probe and the cell surface. The large range reflects real differences among the eggs because these small variations in probe-membrane distance (100–400 μm) never gave such large differences when studied on a single egg. These differences seem to depend on, among other things, the shape and form the furrow takes as cleavage proceeds. In any event, outward current is always recorded opposite new membrane in the cleavage furrow.

When the fertilization envelope was left in place, outward current was detected at the equator 5–10 min after the shallow groove had advanced to the equatorial region of the egg and new membrane was present. The mean maximum outward current was 0.52 ± 0.14 (SD n = 16) μA/cm^2 measured 60 μm from the fertilization envelope.

Inward Current at the First Cleavage Furrow during Second Cleavage

When the fertilization envelope is removed, the animal pole furrow opens up to expose new membrane down to just above the equator of the egg (as shown in Fig. 1*B*). While unpigmented membrane is present at the vegetal furrow, much less new membrane is exposed in the vegetal hemisphere so that the exposed surface membrane at the furrow below the equator of the egg is primarily old membrane. We observed an inward current at this region that was greatest near the end of first cleavage and remained inward as second cleavage began.

A number of measurements were made at the first cleavage furrow during the interval between 10 min before and 10 min after second cleavage started. The measurements were made at the equator with the direction of vibration in the cleavage plane and the probe positioned at the intersection of the cleavage plane and the vertical plane tangent to each edge of the forming blastomeres (as illustrated in Fig. 3*A*, probe positions 5 and 5′). At this location the probe is opposite old, pigmented membrane and 150 μm or more from the nearest cell surface. Between 10 min before second cleavage and 10 min after, the mean inward current at this location was 0.35 ± 0.23 (SD, n = 9) μA/cm^2. When the probe was positioned in the furrow, as in Fig. 3*A*, positions 4 and 4′, the magnitude of the recorded current increased. Current at the equator opposite old, pigmented membrane at the first furrow remains inward during the period of second cleavage. As during first cleavage outward current could only be detected near newly inserted membrane above the equator. When the probe was positioned to the side of the furrow (for example, position 6 and 6′ in Fig. 3*A*) the inward current was much less than at the furrow, the mean being 0.06 ± 0.04 (SD, n = 20).

The larger apparent inward current measured opposite the furrow suggests that the inward current is greater at old membrane which is closer to the new membrane at the furrow. Alternatively the apparent current measured in the furrow may be greater due to the geometry of the furrow and its effect on the current densities. In an effort to distinguish between these two possibilities, we made measurements with the direction of probe vibration exactly perpendicular to the cell surface in the furrow rather than with the direction of probe vibration in the cleavage plane at an angle to the cell surface. Inward current opposite old membrane, measured at the equator of the egg, decreased by a factor of about ⅓ for every 100 μm from the center of the furrow region. An example is shown in Fig. 4*A*. Note that the probe and egg were carefully positioned so that the probe vibrated exactly perpendicular to the membrane surface. For all the measurements of this type the magnitude of the inward current at 200 μm from the furrow center at the equator is reduced to 0.66 ± 0.20 of the magnitude at 100 μm from the furrow center (45 measurements on six eggs, 5–11 measurements per egg). Current magnitude at a distance of 300 μm from the furrow center is further reduced to 0.42 ±0.22 of the magnitude at 100 μm (34 measurements on six eggs, three to eight measurements per egg). Therefore the larger current magnitudes recorded opposite the cleavage furrow in the plane of cleavage are due to a real increase in current density at membrane closer to the center of the furrow region and may also be due in part to the shape of the egg.

The data indicate that current always enters the old, pigmented membrane, but that it does not appear to enter uniformly. The magnitude of the current is largest at the old membrane closer to the new membrane at the furrow region. Fig. 4*B* shows a sketch of the current pattern oberved when the fertilization envelope is removed and the egg is allowed to divide. Such a non-uniform inward current at the old membrane would not result from the resistance to current flow in the extracellular medium since the resistance through a 100 μm high by 250 μm long fluid layer at the egg surface is on the order of a few ohms while the resistance of the membrane region below this fluid is several orders of magnitude greater. Therefore the higher inward current density adjacent to the new membrane suggests a higher concentration of open ion channels in that region of the old membrane. The average currents measured at the first cleavage furrow during first and second cleavage are summarized in Table I and Fig. 5.

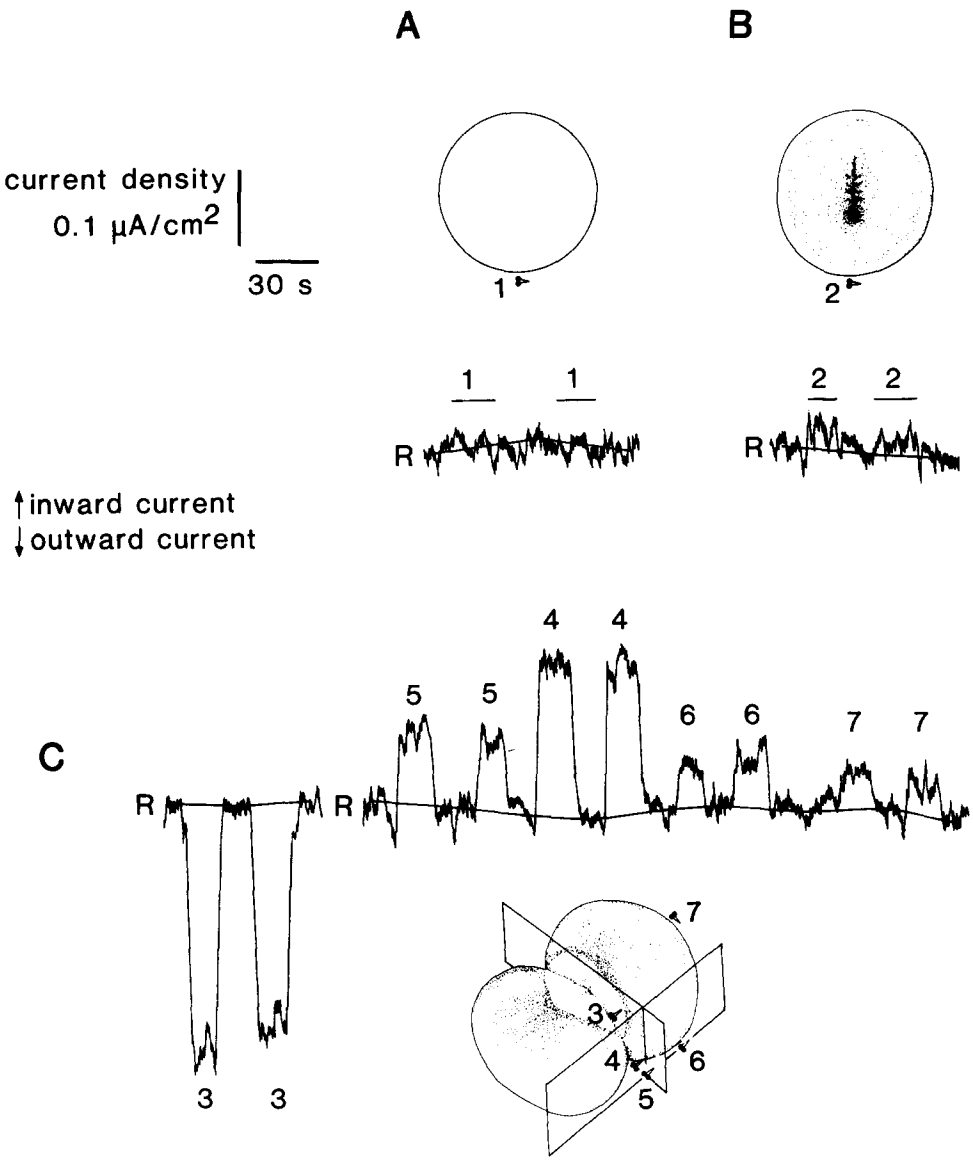

FIGURE 2 Representative recordings of currents in the cleaving *Xenopus* egg with jelly and fertilization envelope removed. Upward deflection from the baseline (*R*) indicates a net influx of positive ions (or net efflux of negative ions) and a downward deflection indicates a net efflux of positive ions (or influx of negative ions). The baseline reference is obtained by moving the probe far from the egg to a reference position outside of the egg's detectable electrical field. Distances from the cell surface are measured from the probe's center point of vibration. (*A*) Record obtained by placing the probe 60 μm from a glass bead similar in size to a dejellied *Xenopus* egg (position *1*). The average signal detected was 0.01 ± 0.02 μA/cm² (SD, $n = 27$) indicating no significant barrier artifact. (*B*) Current recording made from an egg which has just begun to cleave as indicated by the start of surface contraction at the animal pole. The probe was positioned at the equator of the egg and 60 μm from the cell surface (position *2*). (*C*) Current recordings made during first cleavage (just before second cleavage) on the same egg as in *B*, 28 min later. The probe was placed in the following positions: (*3*) opposite the first cleavage furrow 300 μm above the equator and in 270 μm from the vertical plane tangent to the edges of both forming blastomeres with the direction of vibration in the plane of cleavage (~150 μm from the cell surface); (*4*) vibrating in the direction of the cleavage plane at the equator and into the furrow 100 μm from the vertical plane tangent to the edges of both blastomeres (about 100 μm from the cell surface); (*5*) at the equator opposite the furrow aligned with the vertical plane tangent to the edges of both blastomeres with the direction of vibration in the cleavage plane and 150–250 μm from the nearest cell surface on either side of the furrow; (*6*) opposite the right blastomere 60 μm from the cell surface at the equator with the direction of vibration perpendicular to the surface; (*7*) at the side of the right blastomere 60 μm from the cell surface at the equator with the direction of vibration perpendicular to the surface. The break in the recording after the last measurement at position *3* is 3 min.

Steady Ion Currents at the Second Cleavage Furrow

The current pattern at the second cleavage furrow is similar to that described for the first cleavage furrow. This is illustrated by the current recordings shown in Fig. 3*B*. After new membrane is inserted into the plane of second cleavage outward current is detected opposite the new membrane as illustrated in Fig. 3*B*, probe position 8. Inward current is also detected at the second cleavage furrow but only at old, pigmented membrane. Inward current is greatest at the furrow below the area where new membrane is most exposed (as in

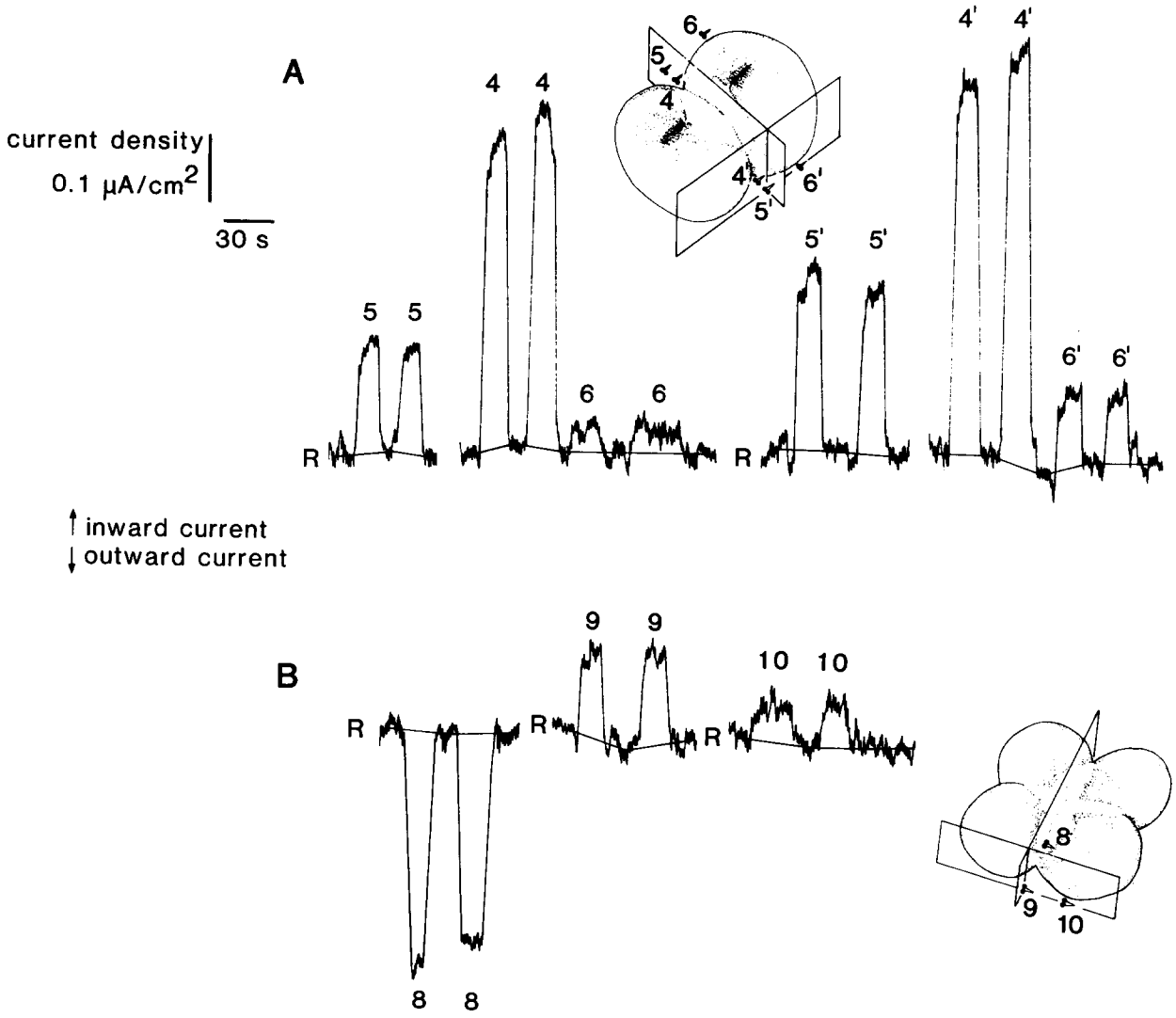

FIGURE 3 Representative recordings made during second cleavage on the same embryo, in both *A* and *B*. (*A*) Current recording made just after second cleavage had started. All measurements made at the equator of the egg below the region of exposed new membrane and opposite old, pigmented membrane at the following positions: 4 and 4′ in the cleavage furrow vibrating in the direction of the cleavage plane and in 160 μm from the vertical plane tangent to the edges of both blastomeres; 5 and 5′ are opposite the first furrow at the intersection of the cleavage plane and the vertical plane tangent to both blastomeres with the direction of vibration in the cleavage plane; 6 and 6′ are 60 μm from the cell surface of the right hand blastomere with the direction of vibration perpendicular to the surface. The break between measurements at 5 and 4 is 1 min, between 6 and 5′ is 0.5 min, and between 5′ and 4′ is 2 min. (*B*) Current recording made during second cleavage on the same egg as in *A*, 6 min later. The probe was placed in the following positions: (*8*) opposite the second cleavage furrow vibrating in the plane of cleavage 300 μm above the equator and in 330 μm from the vertical plane tangent to both of the forming blastomeres ~100 μm from the nearest cell surface; (9) vibrating in the plane of the second cleavage furrow at the equator and at the intersection of the cleavage plane and the vertical plane tangent to each forming blastomere approximately 300 μm to the nearest cell surface; (*10*) opposite the lower right blastomere at the positions indicated, at the equator 60 μm from the cell surface with the direction of vibration perpendicular to the cell surface.

Fig. 3*B*, probe position 9). When the fertilization envelope was left intact a mean maximum outward current of 0.45 ± 0.15 (SD, n = 10) μA/cm² was measured at the equator 60 μm from the fertilization envelope opposite the second cleavage furrow.

Measurements before First Cleavage

The first appearance of large steady currents in the fertilized *Xenopus laevis* egg does not occur until new membrane is inserted in the plane of division during first cleavage. However, we began measurements as early as 15 min after fertilization and between this time and first cleavage we sometimes measured a small inward current. This is illustrated in Fig. 2*B*. The apparent inward current measured before first cleavage may be due to barrier artifacts as described in the materials and methods section. The inward current measured 60 μm from the surface of an uncleaved egg was 0.02 ± 0.02 (SD, n = 22) μA/cm². This is not significantly different from the average inward current of 0.01 ± 0.02 (SD, n = 27) μA/cm² measured near the surface of a glass bead which is due to artifact. It may also be possible that the probe itself induces a very small inward current. This is suggested by the fact that no outward currents were measured at the surface of an uncleaved egg. If a small inward current is induced by the

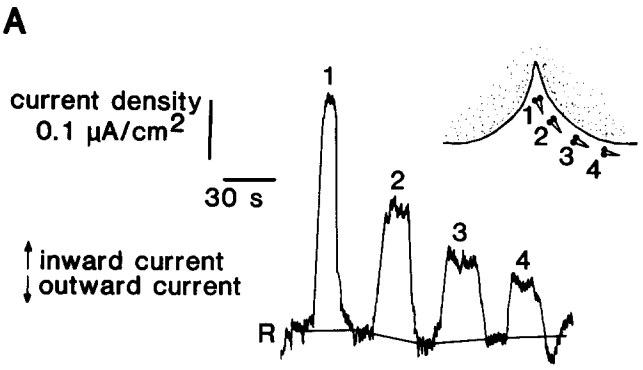

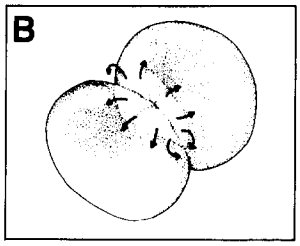

FIGURE 4 (*A*) Representative recordings of currents at the first cleavage furrow opposite old, pigmented membrane in 100-μm steps from the center of the furrow. For each measurement, the probe was positioned at the equator, 60 μm from the cell surface with the direction of vibration perpendicular to the surface. (*B*) Sketch of the current pattern in a *Xenopus* egg during first cleavage with the fertilization envelope removed. Current is represented by arrows leaving the area of new membrane and entering primarily at nearby pigmented membrane.

probe it would have little effect on the much larger currents measured during cleavage.

We could not detect measurable steady currents crossing the plasma membrane during the time of grey crescent formation and the associated dorsal-ventral axis determination. There also appears to be no detectable transcellular current associated with the two surface contraction waves that begin ~20 min before first cleavage (as described by Hara et al. [13]).

Ionic Composition of the Cleavage Current

We have begun to obtain some information about the ionic composition of the steady current at cleavage by altering the ionic composition of the external medium and by the addition of some common ion channel blockers to the medium. Following a change in medium, the probe was returned from the reference position several millimeters away to the same position it was in prior to the medium change. However, the egg changes shape during cleavage, particularly at the furrow, and the probe-membrane distance may have changed slightly during some experiments. Since current magnitude falls off with distance from the surface, small differences in probe-membrane distance may be reflected in an apparent change in the recorded current magnitude. The data for these experiments are summarized in Table II. There is some variation in the data which may be due to small changes in probe-membrane distance or to differences in individual egg response to a change in medium. Nevertheless, the data give some indication of the ionic composition of the inward and outward currents. The vibrating probe measures current at only one location and so cannot measure both inward and outward current simultaneously. The data in Table II indicate changes in either inward or outward current and a change recorded for one direction must reflect an equivalent change in the other direction.

K^+ INVOLVEMENT: A number of experiments were designed to test the hypothesis that K^+ efflux carries the outward current leaving newly inserted membrane. First, extracellular K^+ was removed from the medium and replaced with Na^+ (changing the Na^+ concentration by <2%). Under these conditions the current magnitude increased in five of eight ex-

TABLE I

Magnitude of Currents during First and Second Cleavage

Measurement	Fertilization envelope present	Mean current* ±SD (*n*)
		μA/cm²
Artifact test 60 μm from glass ball. See Fig. 5A.		+0.01 ± 0.02 (27)
0–20 min before first cleavage at the equator 60 μm from the cell surface with the direction of vibration perpendicular to the surface. See Fig. 5B.	No	+0.02 ± 0.02 (22)
1st cleavage furrow at the equator 60 μm from fertilization envelope 0–15 min before second cleavage with the direction of vibration perpendicular to the cell surface. See Fig. 5C.	Yes	−0.52 ± 0.14 (16)
1st cleavage furrow 300 μm above the equator, 100–400 μm from the new membrane surface at furrow center 0–15 min before second cleavage with the direction of vibration in the cleavage plane. See Fig. 5D.	No	−0.43 ± 0.26 (29)
45–90° from the plane of first cleavage, 60 μm from the old membrane surface with the direction of vibration perpendicular to the surface, 0–15 min before second cleavage. See Fig. 5E.	No	+0.06 ± 0.04 (20)
1st cleavage furrow at the equator, in the plane tangent to both blastomeres, with the direction of vibration in the cleavage plane, between 10 min before second cleavage and 10 min after the onset of second cleavage. See Fig. 5F.	No	+0.35 ± 0.23 (15)
2nd cleavage furrow at the equator 60 μm from fertilization envelope with the direction of vibration perpendicular to the surface. See Fig. 5G.	Yes	−0.45 ± 0.15 (10)

* A "+" sign indicates a net influx of positive ions or net efflux of negative ions. A "−" sign indicates a net efflux of positive ions or net influx of negative ions. The mean current is obtained from the largest currents measured at each position on each egg studied. The number of eggs from which recordings were made is indicated in parentheses.

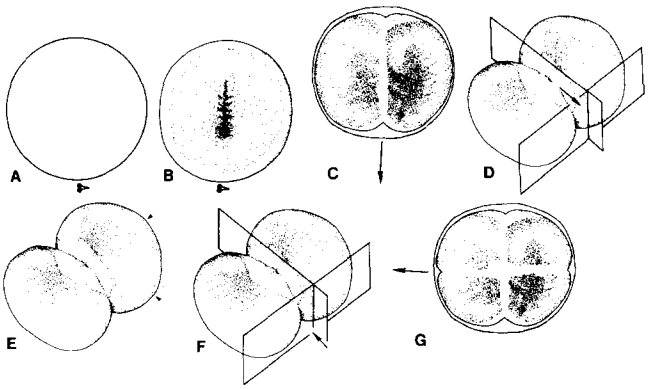

FIGURE 5 See Table I for details.

periments and decreased in three experiments. The average indicates a small increase in current though the data is quite variable. When extracellular K^+ was increased to five times its original concentration (with a reduction in Na^+ of 5%), the magnitude of the current decreased by 42%. It is not likely that these changes are due to the small change in extracellular Na^+ concentration. These results suggest that K^+ is involved in the outward current, however, the results of these experiments are difficult to interpret since a change in external K^+ will change both membrane potential and the K^+ concentration gradient. If the egg's conductance were due mainly to K^+ channels, no change in the total driving force on K^+ would result from this K^+ removal and no change in the current would be expected. Additional experiments were done to study the involvement of K^+ ion in the current. These made use of K^+ channel blockers. The K^+ channel blocker tetraethylammonium ion (14) was added to the extracellular medium at 5 and 15 mM. Neither addition had a significant effect on the current. However, when 1.0 mM $BaCl_2$ was added to the medium the outward current, measured opposite new, unpigmented membrane decreased to zero and in fact reversed direction in all cases. Ba^{2+} has been shown, in a number of systems, to decrease K^+ conductance when applied externally (1, 17, 40). These results suggest that K^+ efflux may be a major component of the outward current associated with new, unpigmented membrane in the furrow region.

Cl^- INVOLVEMENT: The results of two different experiments suggest that Cl^- may carry part of the inward current. (*a*) The replacement of extracellular Cl^- with the impermeant methanesulfonate anion resulted in a increase in the inward current in four out of five experiments, the average being a 70% increase. This reduction in external Cl^- would be expected to reduce Cl^- influx and thus increase net efflux. (*b*) It has been shown that the Cl^- efflux that occurs at fertilization in *Xenopus* can be greatly reduced by the addition of 1.0 mM 4,4′-diisothiocyano-2,2′-stilbene disulfonic acid (DIDS)[1] (43). This indicates that DIDS is effective in blocking electrogenic Cl^- efflux in addition to inhibiting anion exchange as shown in red blood cells (6). The addition of 1 mM DIDS reduces the inward current by 65%, suggesting that Cl^- efflux may be responsible for some of the inward current.

Ca^{++} AND Na^+ INVOLVEMENT: Addition of the Ca^{2+} channel blockers Mn^{2+} or Co^{2+} (reviewed by Hagiwara and Byerly [16]) resulted in a reduction of the current. Addition of 2.0 mM $MnCl_2$ decreased the current to 42% of its original value. When 1.0 mM $CoCl_2$ was added the current magnitude decreased to 52% of the original value. These experiments suggest that Ca^{2+} is involved in the inward current. The involvement of Na^+ influx was implicated by the decrease in the current after the removal of external Na^+ (replacing with choline).

Changes in the current on addition of the chloride salts of Ba^{2+}, Co^{2+}, and Mn^{2+} might also be due to the increase in extracellular Cl^- ion concentration. Increasing the extracellular Cl^- concentration might be expected to decrease the inward current resulting form Cl^- efflux. However, when 4.0 mM choline chloride was added extracellularly, the average current recorded showed a small increase rather than decreasing. This indicates that the decreases in current when $BaCl_2$, $CoCl_2$, and $MnCl_2$ were added to the medium were due to the addition of the cations and not due to the increase in extracellular chloride. It should also be noted that changes in the concentration of extracellular ions are not likely to alter intracellular ion concentrations in these rather impermeable eggs during the time course of these experiments.

EVIDENCE AGAINST A DIRECT Na^+,K^+-ATPASE INVOLVEMENT IN THE CURRENT: Addition of 1.0 mM ouabain, an inhibitor of the Na^+,K^+-ATPase, to the extracellular medium resulted in an average 30% decrease in the outward current. However, Messenger and Warner (27) have noted that at high concentrations between 1.0 and 10.0 mM cardiac glycosides may have some detergent-like effects on cells. If so, records made in 1.0 mM ouabain may be in error due to nonspecific ion leaks. Therefore, we also added ouabain

TABLE II

Experiments to Determine the Ionic Composition of the Current

Medium* changes	Change in current	Ia/Ib‡ (average SD, *n*)
+1.0 mM $BaCl_2$	Decreased to 0 and reversed	−0.53 ± 0.28 (5)
K^+-free	Small increase	1.05 ± 0.60 (8)
Five times K^+ with reduction in Na^+	Decreased	0.58 ± 0.01 (3)
Cl^--free	Increased	1.70 ± 0.67 (5)
+1.0 mM DIDS	Decreased	0.35 ± 0.26 (4)
+2.0 mM $MnCl_2$	Decreased	0.42 ± 0.07 (4)
+1.0 mM $CoCl_2$	Decreased	0.52 ± 0.15 (3)
Na^+-free	Decreased	0.32 ± 0.26 (5)
+4.0 mM choline chloride	Increased	1.26 ± 0.39 (4)
+1.0 mM ouabain	Decreased	0.69 ± 0.23 (4)
+0.01 mM ouabain	No change	1.00 ± 0 (3)
+0.01 mM strophanthidin	Small increase	1.09 ± 0.16 (3)

* Normal medium was 5% De Boer's Saline: 5.50 mM NaCl, 0.07 mM KCl, 0.07 mM $CaCl_2$, and 2.00 mM Tricine. Na^+-free was made with 5.50 mM choline chloride substituted for NaCl, K^+-free with 0.07 mM NaCl for KCl, and Cl^--free with methanesulfonate for chloride. Five times K^+ was made by adding 0.28 mM KCl and reducing NaCl by 0.28 mM (a 5% change in NaCl concentration). Other media were made without substitution by the addition of the chloride salts of barium, cesium, manganese, or cobalt. The Na^+,K^+-ATPase inhibitors, ouabain or strophanthidin were added to 5% De Boer's.

‡ Ratio of the current magnitude after the change in medium (Ia) to the current magnitude in 5% De Boer's solution (Ib). Values >1 indicate an increase in current and values between 0 and 1 indicate a decrease in current. Values <0 indicate that the current fell to zero and then reversed direction (as outward current changing to inward). Values between 0 and −1 indicate that the magnitude of the reversed current was less than that before reversal.

[1] *Abbreviations used in this paper:* DIDS, 4,4′-diisothiocyano-2,2′-stilbene disulfonic acid.

at a reduced concentration which is still effective in inhibiting the Na^+,K^+-ATPase (27). No change in current magnitude was observed when 0.01 mM ouabain was added to the extracellular medium. Also the addition of the reversible Na^+,K^+-ATPase inhibitor, strophanthidin (32), at a concentration of 0.01 mM resulted in no significant change in the average current magnitude. This strophanthidin concentration is within the effective range for inhibiting the Na^+,K^+-ATPase in amphibian cells (27) and in mammalian erythrocytes (12). These experiments do not rule out the possibility that the Na^+-K^+ pump contributes a small amount to the outward current ($<0.01\ \mu A/cm^2$).

DISCUSSION

New Findings

These results confirm the earlier conclusion based on intracellular electrophysiological observations that the unpigmented membrane introduced into the cleavage furrow in frog eggs has a high K^+ permeability (7, 8, 39; in disagreement with reference 10). An outward current is detected at both the first and second cleavage furrow as soon as new, unpigmented membrane appears in those regions. We present new information on the spatial distribution of the steady inward current that indicates a surprising heterogeneity over this equipotential cell (42, 43). Rather than exhibiting a uniform distribution over the old membrane region, the inward current is concentrated at the border of the newly inserted membrane. Preliminary results had suggested that current might enter the prefurrow region ahead of the forming furrow and that such a current might be associated with contractile ring formation (20). However, further measurements have shown that there are no measurable currents during groove formation at the beginning of cleavage. This suggests that if such currents exist, they must be $<0.01\ \mu A/cm^2$. Though not conclusive, our experiments suggest that the inward current may be carried by Na^+ influx, Ca^{2+} influx, and Cl^- efflux. No steady transcellular currents are associated with grey crescent formation or the surface contraction waves preceding cleavage.

Morphology of the Outward Current Region

Several morphological studies of amphibian egg cleavage have suggested that new, unpigmented membrane is added to the cell surface at the cleavage furrow. Surface marking experiments on amphibian eggs have indicated that the new, unpigmented membrane does not form by expansion of the preexisting pigmented membrane (3, 36). Electron microscopy has revealed vesicles or membrane cisternae near the unpigmented membrane (3, 24, 37, 38). It has been suggested that Golgi-derived vesicles may be the source of the new, unpigmented membrane added at the furrow (34).

This unpigmented membrane is morphologically different from the preexisting cell membrane in many respects: (*a*) Thin section electron microscopy indicates that it has a less well-defined trilamellar appearance (3). (*b*) Scanning electron microscopy reveals a smoother surface at the newly added membrane region (3). (*c*) Freeze-fracture electron microscopy indicates a five-fold lower particle density in the new membrane (4, 33). (*d*) At later stages of development, concanavalin A receptors and a cell surface carbohydrate-binding protein or surface lectin are localized to unpigmented membrane (29, 30). Therefore, this new, unpigmented membrane that appears at first cleavage is both morphologically and electrically very different from the original egg membrane.

Localization of Inward Current

The inward current appears to be carried by Ca^{2+} and Na^+ influx and Cl^- efflux in a non-uniform pattern. The inward current at the old membrane bordering the newly inserted membrane is 4 to 30 times larger than that measured farther away from the cleavage furrow. This increase in current density near the furrow region is probably not due to greater membrane folding or concentrated microvilli in the region of the furrow at this stage of development. While a high concentration of microvilli is observed at the prospective furrow before cleavage, as cleavage progresses these become shorter and broader. Only a few microvilli are observed at the furrow region by the end of first cleavage (9).

This non-uniform inward current pattern could be caused by either the concentrating of ion channels in the border region or a nonuniform driving force over the old membrane. This latter possibility is not likely, however, since the parameters that determine driving force, membrane potential and ion concentration gradients, do not exhibit such a non-uniform distribution. The egg is essentially equipotential (42, 43) and no $[Na^+]_i$ gradients have been detected (D. J. Webb and R. Nuccitelli, unpublished results). Therefore, we feel that the inward current distribution probably reflects the non-uniform distribution of ion channels. Due to the rapidly changing curvature of this region during new membrane insertion, it was impossible to measure the current density component normal to this membrane over time in order to determine if this asymmetrical channel distribution developed gradually or was immediately present when the outward current was detected. One appealing possibility is that the tangential electrical field generated by the steady cleavage current acts to laterally electrophorese ion channels toward the border region resulting in an increased channel density there. A steady current of $\sim 1\ \mu A/cm^2$ in 5% De Boer's would generate a tangential electrical field of 0.15 mV/mm along the cell surface. A field of this magnitude could electrophorese charged components in the plane of the membrane (18).

Probable Ionic Composition of the Current

The experiments designed to investigate the ionic composition of the currents suggest that the outward current is carried by K^+ ions. The clearest evidence in support of this comes from those experiments in which $BaCl_2$ was added to the medium. Ba^{2+} reduces the outward current to zero and an apparent reversal of the current is observed. Ba^{2+} decreases K^+ conductance in a number of cells that are insensitive to externally applied tetraethylammonium. Ba^{2+} suppresses the inwardly rectifying K^+ conductance of frog muscle (40) and decreases K^+ conductance in squid giant axon (1). In addition, Ba^{2+} suppresses the delayed rectifier K^+ conductance in amphioxus muscle cells (17). The blocking of K^+ channels at the unpigmented membrane may expose small hidden currents dependent on other ion channels in the new membrane that cannot normally be detected. Ba^{2+} will also enter Ca^{2+} channels readily (16) and this may be an additional factor in the current reversal. We plan to further study this aspect of current reversal and to include experiments to determine how such reversals and other alterations in the natural current might affect development.

These experiments suggest that inward current at the pigmented membrane is carried in part by Na^+ and Ca^{2+} influx. Ca^{2+} has been previously found to regulate membrane permeability in *Xenopus* oocytes and is involved in the prematuration current through these oocytes (31). Cl^- efflux appears to be a component of the inward current at the old, pigmented membrane. Preliminary experiments suggest that the inward current wave crossing the original egg membrane after activation is also carried by Cl^- efflux. Slack and Warner (39) showed that sensitivity to the Na^+,K^+-ATPase inhibitor ouabain was at new membrane facing the blastocoele. Indeed, blastocoele formation was inhibited only when ouabain was injected into the blastocoele cavity. This suggests a localization of the Na^+,K^+-ATPase as found in mouse blastocysts and other epithelia (2, 11, 25, 41). We then therefore looked for the possible localization of the Na^+ pump in *Xenopus* cleavage stage embryos. At first cleavage, with this technique, we do not detect a significant Na^+-K^+ pump contribution to the outward current. However, since the ouabain injection experiments in *Xenopus* were done on 64-cell stage embryos, we plan to look for a Na^+-K^+ pump contribution in these advanced stages.

Development of Epithelial Cell Polarity

The steady currents described here and the electrical properties of the two distinct membranes on which they depend may have a significant role in development. The cleaving *Xenopus* egg quickly begins to form a fluid-filled central cavity or blastocoele at first or second cleavage (24) so the blastomeres are developing into an epithelial layer with an apical side facing the external medium and the basolateral sides bordering adjacent blastomeres and the blastocoele. The new, unpigmented membrane, with its distinct morphology and electrical properties, remains localized at the basolateral region. The steady currents described here are an early indicator of the distinct membrane domains associated with the blastomere's polarity. Even after blastomere disaggregation, outward current remains localized to the new membrane (D. Kline and R. Nuccitelli, unpublished observations) so each blastomere maintains this membrane polarization.

This work was supported by National Science Foundation grant PCM 81 18174 and National Institutes of Health grant K04 HDO 0470-01 to R. Nuccitelli.

Received for publication 27 July 1982, and in revised form 22 August 1983.

REFERENCES

1. Armstrong, C. M., and S. R. Taylor. 1980. Interaction of barium ions with potassium channels in squid giant axons. *Biophys. J.* 30:473–483.
2. Benos, D. J. 1981. Ouabain binding to preimplantation rabbit blastocysts. *Dev. Biol.* 83:69–78.
3. Bluemink, J. G., and S. W. de Laat. 1973. New membrane formation during cytokinesis in normal and cytochalasin B-treated eggs of *Xenopus laevis*. I. Electron microscope observations. *J. Cell Biol.* 59:89–108.
4. Bluemink, J. G., L. G. J. Tertoolen, P. H. J. Ververgaert, and A. J. Verkleij. 1976. Freeze-fracture electron microscopy of preexisting and nascent cell membrane in cleaving eggs of *Xenopus laevis*. *Biochim. Biophys. Acta* 443:143–155.
5. Borgens, R. B., J. W. Vanable, Jr., and L. F. Jaffe. 1979. Bioelectricity and regeneration. *Bioscience* 29:468–474.
6. Cabantchik, Z. I., and A. Rothstein. 1974. Membrane proteins related to anion permeability of human red blood cells. I. Localization of disulfonic stilbene binding sites in proteins involved in permeation. *J. Membr. Biol.* 15: 207–226.
7. de Laat, S. W., and J. G. Bluemink. 1974. New membrane formation during cytokinesis in normal and cytochalasin B-treated eggs of *Xenopus laevis*. *J. Cell Biol.* 60:529–540.
8. de Laat, S. W., R. J. A. Buwalda, and A. M. M. C. Habets. 1974. Intracellular ionic distribution, cell membrane permeability and membrane potential of the *Xenopus* egg during first cleavage. *Exp. Cell Res.* 89:1–14.
9. Denis-Donini, S., B. Baccetti, and A. Monroy. 1976. Morphological changes of the surface of the eggs of *Xenopus laevis* in the course of development. *J. Ultrastruct. Res.* 57:104–112.
10. DiCaprio, R. A., A. S. French, and E. J. Sanders. 1976. On the mechanism of electrical coupling between cells of early *Xenopus* embryos. *J. Membr. Biol.* 27:393–408.
11. Ernst, S. A., and J. W. Mills. 1977. Basolateral plasma membrane localization of ouabain-sensitive sodium transport sites in the secretory epithelium of the avian salt gland. *J. Cell Biol.* 75:74–94.
12. Glynn, I. M. 1957. The action of cardiac glycosides on sodium and potassium movements in human red cells. *J. Physiol. (Lond.).* 136:148–173.
13. Hara, K., P. Tydeman, and M. Kirschner. 1980. A cytoplasmic clock with the same period as the division cycle in *Xenopus* eggs. *Proc. Natl. Acad. Sci. USA.* 77:462–466.
14. Hille, B. 1970. Ionic channels in nerve membranes. *Prog. Biophys. Biophys. Chem.* 21:1–32.
15. Hollinger, T. G., and G. L. Corton. 1980. Artificial fertilization of gametes from the south african clawed frog, *Xenopus laevis*. *Gamete Res.* 3:45–57.
16. Hagiwara, S., and L. Byerly. 1981. Calcium channel. *Annu. Rev. Neurosci.* 4:69–125.
17. Hagiwara, S., and Y. Kidokoro. 1971. Na and Ca components of action potential in amphioxus muscle cells. *J. Physiol. (Lond.).* 219:217–232.
18. Jaffe, L. F. 1977. Electrophoresis along cell membranes. *Nature (Lond.).* 265:600–602.
19. Jaffe, L. F. 1979. Control of development by ionic currents. *In* Membrane Transduction Mechanisms. Cone, R. A., and J. E. Dowling, editors. Raven Press, New York. 199–231.
20. Jaffe, L. F. 1981. The role of ionic currents in establishing developmental pattern. *Phil. Trans. R. Soc. Lond. B Biol. Sci.* 295:553–566.
21. Jaffe, L. F., and R. Nuccitelli. 1974. An ultrasensitive vibrating probe for measuring steady extracellular currents. *J. Cell Biol.* 63:614–628.
22. Jaffe, L. F., and R. Nuccitelli. 1977. Electrical controls of development. *Annu. Rev. Biophys. Bioeng.* 6:445–476.
23. Jaffe, L. F., and C. D. Stern. 1979. Strong electrical currents leave the primitive streak of chick embryos. *Science (Wash. DC).* 206:569–571.
24. Kalt, M. R. 1971. The relationship between cleavage and blastocoel formation in *Xenopus laevis*. II. Electron microscope observations. *J. Embryol. Exp. Morphol.* 26:51–66.
25. Louvard, D. 1980. Apical membrane aminopeptidase appears at site of cell-cell contact in cultured kidney epithelial cells. *Proc. Natl. Acad. Sci. USA.* 77:4132–4136.
26. Luchtel, D., J. G. Bluemink, and S. W. de Laat. 1976. The effect of injected cytochalasin B on filament organization in the cleaving egg of *Xenopus laevis*. *J. Ultrastruct. Res.* 54:406–419.
27. Messenger, E. A., and A. E. Warner. 1979. The function of the sodium pump during differentiation of amphibian embryonic neurones. *J. Physiol. (Lond.).* 292:85–105.
28. Nuccitelli, R. 1978. Ooplasmic segregation and secretion in the *Pelvetia* egg is accompanied by a membrane-generated electrical current. *Dev. Biol.* 62:13–33.
29. Roberson, M. M., and P. B. Armstrong. 1979. Regional segregation of con A receptors on dissociated amphibian embryo cells. *Exp. Cell Res.* 122:23–29.
30. Roberson, M. M., and P. B. Armstrong. 1980. Carbohydrate-binding component of amphibian embryo cell surfaces: restriction to surface regions capable of cell adhesion. *Proc. Natl. Acad. Sci. USA.* 77:3460–3463.
31. Robinson, K. R. 1979. Electrical currents through full-grown and maturing *Xenopus* oocytes. *Proc. Natl. Acad. Sci. USA.* 76:837–841.
32. Sachs, J. R. 1974. Interaction of external K, Na, and cardioactive steroids with the Na-K pump of human red blood cells. *J. Gen. Physiol.* 63:123–143.
33. Sanders, E. J., and R. A. Dicaprio. 1976. A freeze-fracture and concanavalin A-binding study of the membrane of cleaving *Xenopus* embryos. *Differentiation.* 7:13–21.
34. Sanders, E. J., and P. K. Singal. 1975. Furrow formation in *Xenopus* embryos. *Exp. Cell Res.* 93:219–224.
35. Selman, G. G., and M. M. Perry. 1970. Ultrastructural changes in the surface layers of the newt's egg in relation to the mechanism of its cleavage. *J. Cell Sci.* 6:207–227.
36. Selman, G. G., and C. H. Waddington. 1955. The mechanism of cell division in the cleavage of the newt's egg. *J. Exp. Biol.* 32:700–733.
37. Singal, P. K., and E. J. Sanders. 1974. An ultrastructural study of the first cleavage of *Xenopus* embryos. *J. Ultrastruct. Res.* 47:433–451.
38. Singal, P. K., and E. J. Sanders. 1974. Cytomembranes in first cleavage *Xenopus* embryos. *Cell Tissue Res.* 154:189–209.
39. Slack, C., and A. E. Warner. 1973. Intracellular and intercellular potentials in the early amphibian embryo. *J. Physiol. (Lond.).* 232:313–330.
40. Standen, N. B., and P. R. Stanfield. 1978. A potential- and time-dependent blockade of inward rectification in frog skeletal muscle fibres by barium and strontium ions. *J. Physiol. (Lond.).* 280:169–191.
41. Vorbrodt, A., M. Konwinski, D. Solter, and H. Koprowski. 1977. Ultrastructural cytochemistry of membrane-bound phosphatases in mouse embryos. *Dev. Biol.* 55:117–134.
42. Webb, D. J., and R. Nuccitelli. 1981. Direct measurement of intracellular pH changes in *Xenopus* eggs at fertilization and cleavage. *J. Cell Biol.* 91:562–567.
43. Webb, D. J., and R. Nuccitelli. 1982. Intracellular pH changes accompanying the activation of development in frog eggs: comparison of pH microelectrodes and ^{31}P-NMR measurements. *In* Intracellular pH: Its Measurement, Regulation, and Utilization in Cellular Functions. R. Nuccitelli and D. Deamer, editors. Alan R. Liss, Inc., New York. 293–324.
44. Woodruff, R. I., and W. H. Telfer. 1980. Electrophoresis of proteins in intercellular bridges. *Nature (Lond.).* 286:84–86.
45. Woodward, D. J. 1968. Electrical signs of new membrane production during cleavage of *Rana pipiens* eggs. *J. Gen. Physiol.* 52:509–531.